

Synthesis and Application of r-rhuEPO/NiO/CNTs modified Glassy Carbon Electrode as Sensor for Determination of Erythropoietin in the Blood of Athlete

Furong Duan

Department of Physical Education Teaching, Sichuan Vocational & Technical College, Suining, 629000, China

E-mail: duanfurong323@163.com

Received: 3 September 2021 / Accepted: 9 October 2021 / Published: 10 November 2021

The goal of this research was to create an electrochemical biosensor based on reduced-rhuEPO on NiO nanoparticles (NiO NPs) decorated carbon nanotubes (r-rhuEPO/NiO/CNTs) for easy rhuEPO determination in human blood plasma. For synthesis of electrochemical biosensor, the activated CNTs and NiO NPs were electrodeposited on GCE surface, respectively. The chronoamperometry was used for reduction rhuEPO and modified NiO/CNTs/GCE with reduced-rhuEPO (r-rhuEPO/NiO/CNTs/GCE). The results of structural analyses using SEM and XRD showed that NiO NPs were heterogeneously decorated on the surface of CNTs/GCE which formed highly porous and large active surface area which enhanced the electrochemical activity of electrodes and charge transfer rate. The electrochemical studies using DPV technique showed that r-rhuEPO/NiO/CNTs/GCE was sensitive and stable rhuEPO biosensor with linear range of 100–1300 ng/l and limit of detection of 0.02 ng/l. The applicability of the r-rhuEPO/NiO/CNTs/GCE as rhuEPO biosensor in athlete's blood plasma as a real sample was investigated and results indicated the obtained values for recovery (95.66% to 99.50%) and RSD (2.12% to 3.33%) were acceptable, and the proposed method can applied as practical rhuEPO biosensor for blood plasma samples.

Keywords: CNTs; NiO nanoparticles; Electrodeposition; Erythropoietin; Differential pulse voltammetry

1. INTRODUCTION

Erythropoietin (EPO), also called hematopoietic or hemopoietin, is a glycoprotein cytokine and hormone that aids in the formation of red blood cells, which transport oxygen from the lungs to the rest of the body [1]. When oxygen levels in the cells are low and cellular hypoxia occurs, the kidneys and liver create EPO [2]. The hormone then stimulates the bone marrow, which, in turn, makes more red blood cells [3]. Excess EPO is caused by persistent low-oxygen exposure or rare malignancies, as well

as hypoxemia caused by chronic lung illness, which produces high levels of EPO [4]. It causes a condition known as polycythemia which means high red blood cell count. Right-to-left cardiac shunts or high altitude also can result in EPO production [5]. Weakness, weariness, headache, itching, joint discomfort, and dizziness are some of the generic and non-specific symptoms [6].

Exogenous erythropoietin, also known as recombinant human erythropoietin (rhuEPO), is a biopharmaceutical that is produced in cell culture using recombinant DNA technology. Erythropoiesis-stimulating agents are used to treat anemia in chronic kidney disease, myelodysplasia, and cancer chemotherapy-induced anemia. Because raising hemoglobin levels from 11g/dL to 12g/dL might result in mortality, myocardial infarction, stroke, venous thromboembolism, and tumor recurrence, hemoglobin levels must be closely monitored during EPO treatment [7].

Red blood cells shuttle oxygen to cells, including muscle cells, allowing them to perform more effectively. This is why athletes use rhuEPO. The drug is prohibited in sports since it is thought to improve an athlete's performance and provide those who use it an unfair edge over those who do not use it. Furthermore, EPO thickens a person's blood, thus increasing the risk of clots [8].

Therefore, many studies have been focused on the synthesis, identification and determination the rhEPO level in human blood plasma such as high-performance liquid chromatography [9], immunochromatography [10], affinity probe capillary electrophoresis [11], fluorescence [11], Raman [12], radioimmunoassay [13], and electrochemical techniques [14-16]. Between these determination methods, electrochemical techniques have shown great interest in a wide range of clinical diagnostics because of low cost, sensitivity and selectivity [17-20]. Furthermore, studies have indicated the capability of modification of electrodes in these techniques using nanostructured hybrids and composites can improve the stability, repeatability and sensitivity [14-16, 21]. Therefore, this study was carried out on synthesis of electrochemical sensors based on r-rhuEPO/NiO/CNTs/GCE for facile determination of rhuEPO in the human blood plasma.

2. MATERIALS AND METHOD

2.1. *Synthesize the modified electrodes*

Before the electrodeposition, a GCE surface was sequentially polished using alumina slurry (99.9%, nanoshel, UK) on a micro-cloth pad (Buehler, Germany) until to obtain mirror-like surface, and then GCE was ultrasonically rinsed with deionized (DI) water and ethanol for 10 minutes, respectively. CNTs (>97%, diameter of 40 μ m, Qingdao Haoyu Graphite Products Co., Ltd., China) were activated through the immersion in with equal volume of HF (48%, Merck, Germany) and HNO₃ (65%, Merck, Germany) overnight. Next, the activated CNTs were washed with DI water repeatedly, and then dried at 300°C for 3 hours. All electrodeposition was performed in an Autolab® PGSTAT30 potentiostat (EcoChemie, The Netherland) using three- electrode electrochemical cell which contained working electrode (GCE or modified GCE), counter electrode (Pt foil) and reference electrode (Ag/AgCl (3M KCl)). Electrodeposition of CNTs on GCE surface (CNTs/GCE) was carried out using 0.3 g/l CNTs suspension at current density of 40 mA/cm² during 1 hours [22, 23]. The electrolyte was stirred using a magnetic stirrer. After then, electrodeposition of NiO NPs on CNTs/GCE

(NiO/CNTs/GCE) was accomplished using electrolyte which 250 g/l NiSO₄·6H₂O ($\geq 99\%$, Sigma-Aldrich), 38 g/l NiCl₂·6H₂O (99.9%, Sigma-Aldrich) and 40 g/L H₃BO₃ ($\geq 99.5\%$, Sigma-Aldrich) at current density of 50 mA/cm² within 1 hours [24].

1 μM rhuEPO (Sigma-Aldrich) as standard solution was prepared in 0.1M phosphate buffer solution (PBS) (pH 7.4). For modified NiO/GCE and NiO/CNTs/GCE with r-rhuEPO (r-rhuEPO/NiO/GCE and r-rhuEPO/NiO/CNTs/GCE), 0.05 ml of standard rhuEPO solution was loaded on modified electrodes, and reduced by chronoamperometry at potential of -0.9 V for 5 to 30 minutes in 0.1M KOH [25].

2.2 Characterization

For electrochemical analyses of rhuEPO, chronoamperometry and differential pulse voltammetry (DPV) measurements using the AUTOLAB electrochemical system in three-electrode electrochemical cell were employed for electrochemical desorption of the reduced protein from the modified electrode surface in 0.1M PBS (pH 7.4) at potential range from -0.6 V to 0.4 V at a scan rate of 20 mV/s. The 0.1M PBS was prepared from an equal volume ratio of 0.1 M NaH₂PO₄ (99%, Sigma-Aldrich) and 0.1 M Na₂HPO₄ ($\geq 99.0\%$, Sigma-Aldrich). The enzyme-linked immunosorbent assay kit (ELISA, optical density at 450 nm, Air Plants Bio., Tokyo, Japan) was used for analyses of rhuEPO in human blood plasma that the concentration range of its calibration plot was in the range of 11 – 334 ng/l. The morphology and crystallographic structures of the electrodeposited nanostructures were investigated using scanning electron microscope (SEM, LEO SUPRA 35 VP, Carl Zeiss, Oberkochen, Germany) and X-ray diffractometer (XRD, Philips X'pert MPD), respectively.

2.3. Preparation the real sample

To make magnetic beads that conjugate the antibody, the mixture was prepared which contained of 0.1 ml of 0.15 M 1-ethyl-3-(3-dimethylaminopropyl) carbodiimide (EDAC, 99%, Sigma-Aldrich), 0.1 ml of 0.15 M N-hydroxysuccinimide (NHS, 98%, Merck, Germany) and 1g Fe₃O₄ NPs coated with 1% polyvinylpyrrolidone (98%, diameter of ~30 nm, US Research Nanomaterials, Inc., USA) under magnetic stirring. Subsequently, 10 μL of 0.1 g/l anti-rhuEPO antibody (Ab, MAIIA Diagnostics, Sweden) was added to the resulting mixture. In order to complete conjugation of magnetic beads with antibodies, the obtained suspension was stored at 4 °C for 3 hours, and then the Ab-conjugated magnetic beads were collected with an external magnet. The Ab conjugated magnetic beads were dispersed in 0.1 ml of 0.1M PBS (pH 7.4) and stored at 4 °C until use.

The Ab-conjugated magnetic beads were applied to selective extraction of rhuEPO from human blood plasma. 10 ng/l of rhuEPO was injected into the rhuEPO free-human blood plasma which was provided from Beijing Tiantan Puhua Hospital, China. Thereupon, 0.1 ml of the Ab-conjugated magnetic beads was added to athlete's blood plasma under magnetic stirring. Then, the sample was left for 20 minutes at 20°C. Eventually, the magnetic beads were magnetically separated from the sample. For remove the absorbed rhuEPO from the conjugated magnetic beads which immersed in the equal

volume ratio of mixture of 0.1 M glycine ($\geq 99\%$, Sigma-Aldrich) and 0.1M KOH ($\geq 99\%$, Sigma-Aldrich) for 6 minutes at 20°C. Then, gravity flow size-exclusion system (GE Healthcare, USA) was used for eliminate the glycine buffer form the released rhuEPO solution. After then, the obtained protein was washed with 0.5ml of 0.1 M KOH. To analyze the rhuEPO in an athlete's blood plasma, 0.05 ml of the washed rhuEPO was loaded onto the modified NiO/CNTs/GCE and dried with a stream of nitrogen gas.

3. RESULTS AND DISCUSSION

3.1. Structural analyses of electrodeposited nanostructures

Figure 1 presents the SEM images of CNTs/GCE, NiO/GCE and NiO/CNTs/GCE. As seen from Figure 1a, CNTs were homogeneously electrodeposited on GCE surface and forms a high porous spaghetti-like network with diameter of ~ 90 nm. As observed from Figure 1b, the electrodeposited NiO NPs on GCE surface displays the homogeneous distribution of NPs in spherical-shape with average diameter of 70 nm. Figure 1c shows that the NiO NPs were heterogeneously decorated on the surface of CNTs/GCE. The random distribution of Ni NPs on CNTs related to the porous surface and numerous defects on electrodeposited CNTs on GCE provide the hot spot place for electrodeposition the NiO NPs. Additionally, the heterogeneous surface of NiO/CNTs/GCE creates a highly porous and large active surface area which enhances the electrochemical activity of electrodes and charge transfer rate [26, 27].

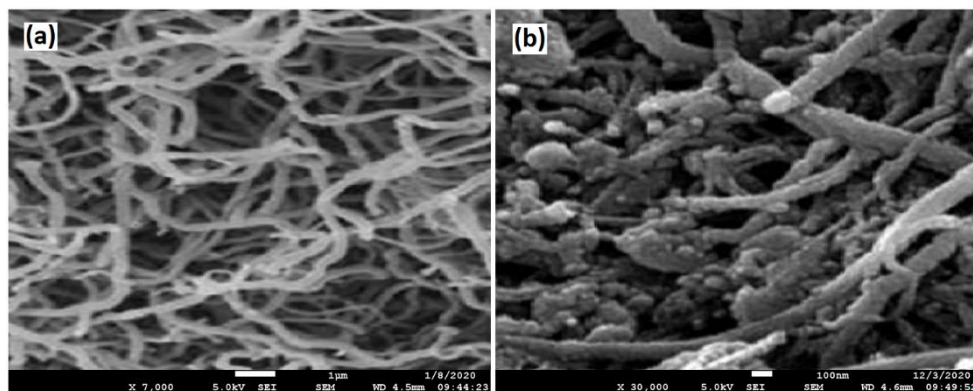


Figure 1. SEM images of (a) CNTs/GCE, (b) NiO/CNTs/GCE.

Figure 2 shows the XRD patterns of powders of electrodeposited CNTs and NiO NPs and NiO/CNTs. The XRD pattern of CNTs in Figure 2a shows two diffraction peaks at 25.97° and 43.11° , corresponding to formation of the graphitic planes of (002) and (1000), respectively. The XRD pattern of NiO NPs and NiO/CNTs in Figures 2b and 2c exhibits the diffraction peaks at 37.29° , 43.54° and 62.97° which related to formation the centered cubic phase of NiO with (111), (200) and (220) planes, respectively (JCPDS card No. 43-1477). The XRD pattern of NiO/CNTs shows the additionally weak peak at 26° which indicates successful electrodeposition of NiO NPs on CNTs.

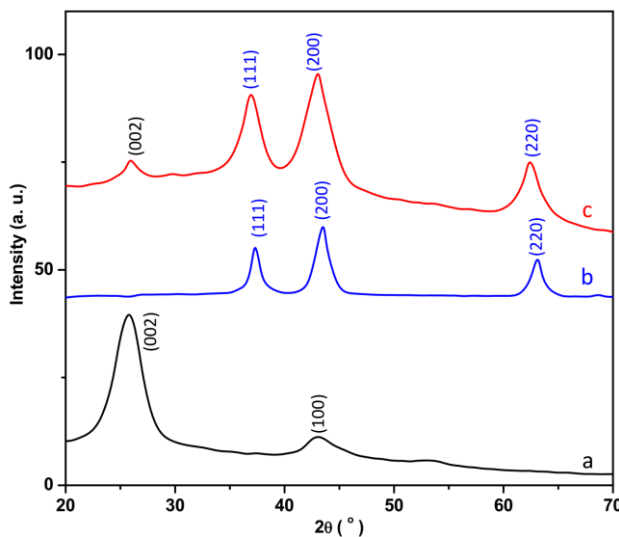


Figure 2. XRD patterns of powders of electrodeposited (a) CNTs and (b)NiO NPs and (c) NiO/CNTs.

3.2. Electrochemical study of biosensor

The normal values of EPO in healthy adults range between 7 and 19 ng/l [28]. Thus, the sensing capability of the electrochemical biosensor of rhuEPO should be investigated within ng/l concentration range. Figure 3 shows the resulted DPV curves of GCE, CNTs/GCE, NiO/GCE, NiO/CNTs/GCE, r-rhuEPO/NiO/GCE and r-rhuEPO/NiO/CNTs/GCE in presence of 10 ng/l rhuEPO in 0.1M PBS (pH 7.4) at scan rate of 20 mV/s. It can be observed from Figures 3a to 3d that there are no redox peaks for desorption of rhuEPO for GCE, CNTs/GCE, NiO/GCE and NiO/CNTs/GCE. The DPV curves of r-rhuEPO/NiO/GCE and r-rhuEPO/NiO/CNTs/GCE in Figures 3e and 3f show the peak current at potential of -0.1V and -0.07V, respectively that related to the electrochemical reduction and entrapment of protein onto the surface of electrodes under 25 minutes chronoamperometry which leads to cleaving the disulfide bond between neighboring protein residues [29, 30]. It resulted in the formation of the free thiol or incomplete disulfide bonding of protein and subsequently the Ni–S π bonding in nickel–cysteine [31, 32]. Moreover, the comparison between DPV curves in Figures 3e and 3f reveals that the peak in r-rhuEPO/NiO/CNTs/GCE possesses a higher current and lower potential than that on r-rhuEPO/NiO/GCE. It can be attributed to porous CNTs frameworks with high electrical conductivity [33-35], and biocompatibility of CNTs with a macroporous structure that increases cellular proliferation and allows the control of the protein activity [33, 36]. Therefore, r-rhuEPO/NiO/CNTs/GCE was selected for following electrochemical studies.

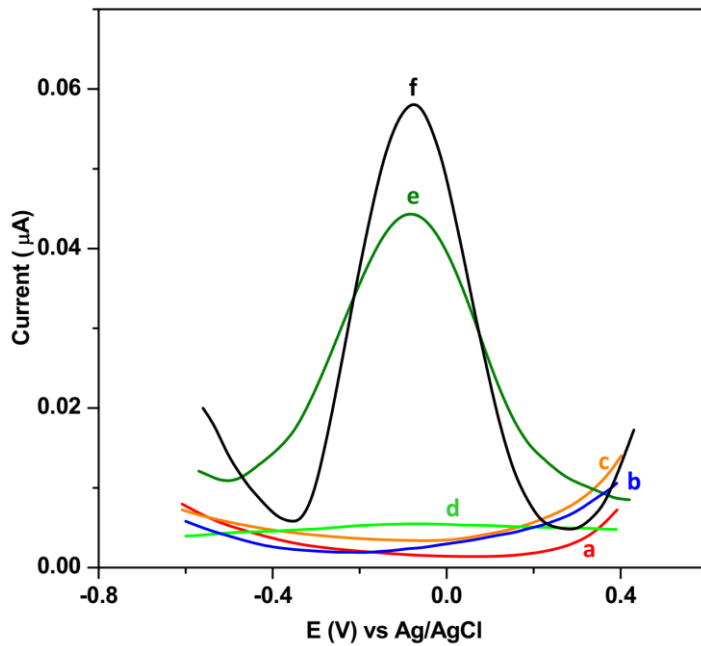


Figure 3. DPV curves of (a) GCE, (b) CNTs/GCE, (c) NiO/GCE, (d) NiO/CNTs/GCE, (e) r-rhuEPO/NiO/GCE and (f) r-rhuEPO/NiO/CNTs/GCE in presence of 10 ng/l rhuEPO in 0.1M PBS (pH 7.4) at scan rate of 20 mV/s.

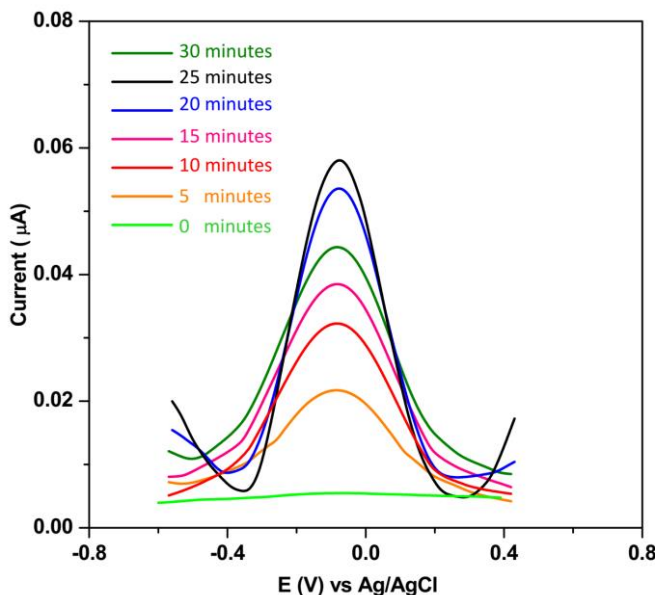


Figure 4. DPV curves of r-rhuEPO/NiO/CNTs/GCE in presence of 10 ng/l rhuEPO in 0.1M PBS (pH 7.4) at scan rate of 20 mV/s after 0 to 30 minutes reduction of rhuEPO through the chronoamperometry.

Further electrochemical measurements were conducted on study of the reduction time effect on sensitivity of electrochemical response of r-rhuEPO/NiO/CNTs/GCE in presence of 10 ng/l in rhuEPO 0.1M PBS (pH 7.4) at scan rate of 20 mV/s. Figure 4a shows the DPV curves of the modified electrode after 0 to 30 minutes reduction of rhuEPO. As seen, the peak current intensity at -0.07V is increased

with increasing the reduction time from 5 to 25 minutes, indicating the enhancement of the amount of immobilized reduced protein on modified electrodes [25]. For a reduction of more than 25 minutes, the peak current value is decreased so that it may be related to more cover of the electroactive sites on the electrode surface. In fact, the conductive electrode surface is covered by non-conductive film [37]. Thus, the 25 minutes reduction time through the chronoamperometry was selected to make the sensitive detection of the protein in following electrochemical measurements.

Figure 5 shows the stability effect of response of r-rhuEPO/NiO/CNTs/GCE toward the 10 ng/l rhuEPO in 0.1M PBS (pH 7.4) at a scan rate of 20 mV/s. It can be observed that the difference between the first and 50th DPV responses shows ~8% decrease which associated with the great stability of response of proposed electrode for determination of rhuEPO because of presence of electrodeposited Ni NPs on the walls and tips of the hollow nanotubes, forming a mesoporous metal-carbon interference. This tip-growth model can facilitate the charge transfer between the biomolecules and mesoporous metal-carbon interference, and more stabilization of biomolecules within the porous structure of modified electrodes [38-40]. The trapped active biomolecules in the porous bundles during 25 minutes of electrochemical reduction of rhuEPO can prevent active material loss and inhibit the shuttle process [41].

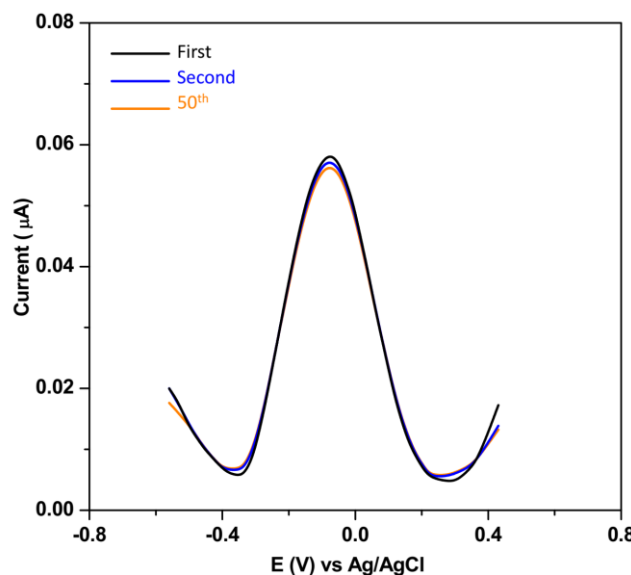


Figure 5. The stability effect of response of r-rhuEPO/NiO/CNTs/GCE toward the 10 ng/l rhuEPO in 0.1M PBS (pH 7.4) at scan rate of 20 mV/s; (a) first, (b) second and (b) 50th DPV responses.

Figure 6 exhibits the DPV responses and calibration plot of r-rhuEPO/NiO/CNTs/GCE to add different concentrations of rhuEPO in 0.1M PBS (pH 7.4) at scan rate of 20 mV/s. As seen, the electrochemical desorption current is linearly increased with increasing the protein content in the range 100–1300 ng/l. For the higher concentration of protein the calibration plot shows the deviation from the linear relationship. The limit of detection was obtained 0.02 ng/l. Furthermore, the results sensing properties in this study is compared with the previously reported rhuEPO sensors in Table 1.

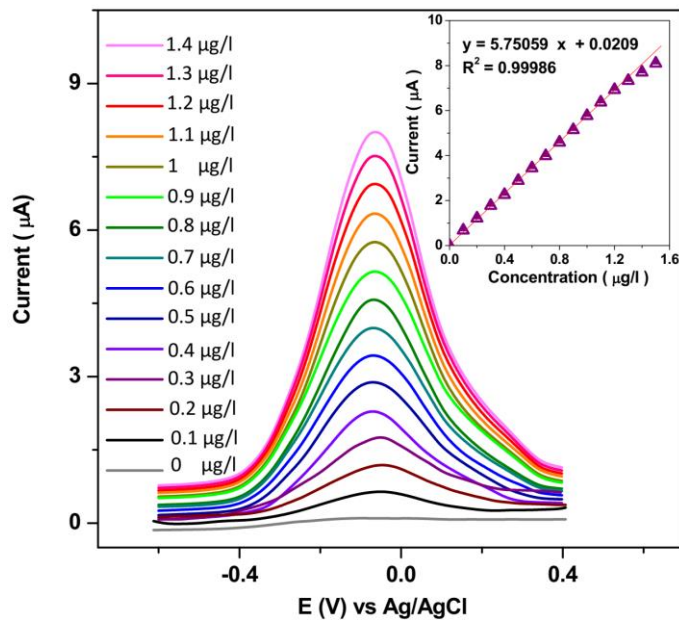


Figure 6. (a) DPV responses and (b) calibration plot of r-rhuEPO/NiO/CNTs/GCE to addition different concentration of rhuEPO in 0.1M PBS (pH 7.4) at scan rate of 20 mV/s.

Table 1. Comparison between the resulted sensing properties of r-rhuEPO/NiO/CNTs/GCE and the previously reported rhuEPO sensors.

Electrode	Sensing technique	Linear range (ng/l)	Detection limit (ng/l)	Ref.
r-rhuEPO/NiO/CNTs/GCE	DPV	100 to 1300	0.02	This work
nano-Au/ZnO sol-gel/nano-Au/GCE	CV	5×10^{-4} to 500	10^{-4}	[14]
Polydopamine imprinted polymer	Potentiometry	10^3 to 10^5	330	[15]
rhEPO/Silica-based rhEPO-molecularly imprinted polymer	RP-HPLC	2×10^4 to 10^5	21240	[9]
Anti-EPO/polyesterbacked nitrocellulose membrane	IMCG	1.7 to 51	0.035	[10]
Single-stranded DNA aptamer probe	APCE/LIF	7×10^3 to 3.5×10^6	7.4×10^3	[11]
mercury electrode	SWV	40 to 400	17	[16]
Anti-EPO /Rod-shaped gold NPs	SERP	0.1 to 10^3	0.1	[12]

SWASV: Square wave anodic stripping voltammetry; RP-HPLC: Reversed-phase of high-performance liquid chromatography; IMCG: Immunochromatography; APCE/LIF: Affinity probe capillary electrophoresis/laser-induced fluorescence; SWV: Square wave voltammetry; SERP: Surface-enhanced Raman probe

It can be observed that the sensor in r-rhuEPO/NiO/CNTs/GCE displays is better than or comparable with that of other reported rhuEPO sensors which related to good catalytic performance of NiO/CNTs frameworks which provides higher specific surface area and anchoring sites for biomolecules and charge transfer channel for catalytic reactions [42].

For investigation the applicability of the r-rhuEPO/NiO/CNTs/GCE as rhuEPO biosensor in athlete's blood plasma as real sample, the rhuEPO were extracted using the polymer-functionalized magnetic beads, reduced on a NiO/CNTs/GCE using chronoamperometry. The selective isolation of rhuEPO from human blood plasma as one of the most complex biological matrices is important in electrochemical sensing. During 1-ethyl-3-(3-dimethylaminopropyl) carbodiimide (EDAC) reaction in synthesis of magnetic beads, EDAC as mediator and crosslinker can reacts with a carboxyl group of antibody results in an active O-acylisourea intermediate which can be easily displaced by a nucleophilic attack from primary amino groups that it forms an amine-reactive intermediate which can covalently conjugate amine group of magnetic beads [43, 44]. Simultaneously, the addition of EDAC/NHS carbodiimide coupling reagents to polyvinylpyrrolidone-functionalized magnetic NPs leads to activation of the primary amines (HN_2 groups) of functionalized magnetic beads [45]. N-hydroxysuccinimide (NHS) as a trapping agent rapidly reacts with the O-acylisourea intermediate creating reactive esters [44]. The NHS ester will then react with the amine on biological agents by covalent attachment of an acyl group to the nucleophile with the release of the NHS leaving group. This EDS/NHS reaction is commonly referred to as a zero-length crosslinking reaction because the crosslinkers catalyze directional bonding between the macromolecules and the polymer but are not present in the final result [44, 46]. Therefore, these activated groups can form a covalent bond of amide that binds to the antibody on the bead surface which can act as a selective agent to extract rhuEPO from human blood plasma [47, 48]. Table 2 shows the quantification results by DPV and ELISA techniques in prepared real sample which implied to the average concentration of rhuEPO in the plasma sample are estimated of 9.02 ng/l and 9.42 ng/l by DPV and ELISA techniques, respectively, indicating the good agreement and accuracy between two techniques. Furthermore, the results of analytical studies by standard addition method through the DPV technique are shown in Table 2.

Table 2. Results of determination of rhuEPO in real blood plasma sample by DPV and ELISA techniques.

DPV					ELISA	
Content in sample (ng/l)	Added (ng/l)	Found (ng/l)	Recovery (%)	RSD (%)	Content in sample (ng/l)	RSD (%)
9.02				2.77	9.42	2.08
	20.0	19.2	96.00	2.12		
	40.0	39.8	99.50	2.68		
	60.0	57.4	95.66	3.24		
	80.0	78.5	98.12	3.33		

It can be found that the obtained values for recovery (95.66% to 99.50%) and relative standard deviation (RSD) (2.12% to 3.33%) are acceptable, and the proposed method can be applied as practical rhuEPO biosensor for blood plasma samples.

4. CONCULUSION

This study was carried out on synthesis of electrochemical biosensors based on r-rhuEPO/NiO/CNTs/GCE for facile determination of rhuEPO in the human blood plasma. The electrodeposition technique was applied for modification of the NiO/CNTs on GCE surface and chronoamperometry was used for reduction rhuEPO on NiO/CNTs/GCE (r-rhuEPO/NiO/CNTs/GCE). The results of structural analyses showed that NiO NPs were heterogeneously decorated on the surface of CNTs/GCE. The electrochemical studies showed that r-rhuEPO/NiO/CNTs/GCE was a sensitive and stable rhuEPO biosensor with linear range of 100–1300 ng/l and limit of detection of 0.02 ng/l. The applicability of the r-rhuEPO/NiO/CNTs/GCE as rhuEPO biosensor in athlete's blood plasma as real sample was investigated and results indicated the obtained values for recovery and RSD were acceptable, and the proposed method can applied as practical rhuEPO biosensor for blood plasma samples.

References

1. A. Merelli, L. Czornyj and A. Lazarowski, *International Journal of Neuroscience*, 125 (2015) 793.
2. H. Karimi-Maleh, M.L. Yola, N. Atar, Y. Orooji, F. Karimi, P.S. Kumar, J. Rouhi and M. Baghayeri, *Journal of colloid and interface science*, 592 (2021) 174.
3. M.J. Koury, *Experimental hematology*, 33 (2005) 1263.
4. B.L. Ebert and H.F. Bunn, *Blood*, *The Journal of the American Society of Hematology*, 94 (1999) 1864.
5. H. Karimi-Maleh, Y. Orooji, F. Karimi, M. Alizadeh, M. Baghayeri, J. Rouhi, S. Tajik, H. Beitollahi, S. Agarwal and V.K. Gupta, *Biosensors and Bioelectronics*, 184 (2021) 113252.
6. Y. Orooji, B. Tanhaei, A. Ayati, S.H. Tabrizi, M. Alizadeh, F.F. Bamoharram, F. Karimi, S. Salmanpour, J. Rouhi and S. Afshar, *Chemosphere*, 281 (2021) 130795.
7. B.D. Bradbury, M.D. Danese, M. Gleeson and C.W. Critchlow, *Clinical Journal of the American Society of Nephrology*, 4 (2009) 630.
8. N. Robinson, S. Giraud, C. Saudan, N. Baume, L. Avois, P. Mangin and M. Saugy, *British journal of sports medicine*, 40 (2006) i30.
9. M.A.A. El-Aal, M.A. Al-Ghobashy and Y.S. El-Saharty, *Journal of Chromatography A*, 1641 (2021) 462012.
10. M. Lönnberg, M. Drevin and J. Carlsson, *Journal of Immunological Methods*, 339 (2008) 236.
11. R. Shen, L. Guo, Z. Zhang, Q. Meng and J. Xie, *Journal of Chromatography A*, 1217 (2010) 5635.
12. Y.S. Selbes, M.G. Caglayan, M. Eryilmaz, I.H. Boyaci, N. Saglam, A.A. Basaran and U. Tamer, *Analytical and Bioanalytical Chemistry*, 408 (2016) 8447.
13. O.J. Nielsen, *Clinica chimica acta*, 176 (1988) 303.

14. L. Zhang, Y. Wang, J. Wang, J. Shi, K. Deng and W. Fu, *Biosensors and Bioelectronics*, 50 (2013) 217.
15. A.H. Nadim, M.A. Abd El-Aal, M.A. Al-Ghobashy and Y.S. El-Saharty, *Microchemical Journal*, 167 (2021) 106333.
16. P. Hernández, O. Nieto and L. Hernández, *Analytica Chimica Acta*, 305 (1995) 340.
17. H. Sun, Z. Jiang, H. Wang and H. Zhao, *International Journal of Electrochemical Science*, 10 (2015) 9714.
18. H. Wang, X. Wu, P. Dong, C. Wang, J. Wang, Y. Liu and J. Chen, *International Journal of Electrochemical Science*, 9 (2014) 12.
19. L. Shan, *International Journal of Electrochemical Science*, 15 (2020) 12587.
20. Z. Savari, S. Soltanian, A. Noorbakhsh, A. Salimi, M. Najafi and P. Servati, *Sensors and Actuators B: Chemical*, 176 (2013) 335.
21. H. Savaloni, E. Khani, R. Savari, F. Chahshouri and F. Placido, *Applied Physics A*, 127 (2021) 1.
22. S. Palisoc, P.G. De Leon, A. Alzona, L. Racines and M. Natividad, *Heliyon*, 5 (2019) e02147.
23. C. Guo, Y. Zuo, X. Zhao, J. Zhao and J. Xiong, *Surface and Coatings Technology*, 202 (2008) 3385.
24. L. Shi, C.F. Sun, P. Gao, F. Zhou and W.M. Liu, *Surface and Coatings Technology*, 200 (2006) 4870.
25. W.A. Hassanain, A. Sivanesan, E.L. Izake and G.A. Ayoko, *Talanta*, 189 (2018) 636.
26. Z. Savari, S. Soltanian, A. Noorbakhsh and A. Salimi, *9th Iranian Annual Seminar of Electrochemistry*, 9 (2013) 1.
27. R. Savari, H. Savaloni, S. Abbasi and F. Placido, *Sensors and Actuators B: Chemical*, 266 (2018) 620.
28. F. Tamion, V. Le Cam-Duchez, J.-F. Menard, C. Girault, A. Coquerel and G. Bonmarchand, *Critical Care*, 8 (2004) R328.
29. X. Zhong and J.F. Wright, *International journal of cell biology*, 2013 (2013) 1.
30. I. Stoian, B. Manolescu, V. Atanasiu and O. Lupescu, *Open Medicine*, 2 (2007) 361.
31. J.C. Way, S. Lauder, B. Brunkhorst, S.-M. Kong, A. Qi, G. Webster, I. Campbell, S. McKenzie, Y. Lan and B. Marelli, *Protein Engineering Design and Selection*, 18 (2005) 111.
32. P.J. Desrochers, D.S. Duong, A.S. Marshall, S.A. Lelievre, B. Hong, J.R. Brown, R.M. Tarkka, J.M. Manion, G. Holman and J.W. Merkert, *Inorganic chemistry*, 46 (2007) 9221.
33. T. Szymbański, A.A. Mieloch, M. Richter, T. Trzeciak, E. Florek, J.D. Rybka and M. Giersig, *Materials*, 13 (2020) 4039.
34. J. Simon, E. Flahaut and M. Golzio, *Materials*, 12 (2019) 624.
35. R. Savari, J. Rouhi, O. Fakhar, S. Kakooei, D. Pourzadeh, O. Jahanbakhsh and S. Shojaei, *Ceramics International*, 47 (2021) 31927.
36. B. Pei, W. Wang, N. Dunne and X. Li, *Nanomaterials*, 9 (2019) 1501.
37. R.D. Crapnell, A. Hudson, C.W. Foster, K. Eersels, B.v. Grinsven, T.J. Cleij, C.E. Banks and M. Peeters, *Sensors*, 19 (2019) 1204.
38. P. Pinyou, V. Blay, L.M. Muresan and T. Noguer, *Materials Horizons*, 6 (2019) 1336.
39. F. Chahshouri, H. Savaloni, E. Khani and R. Savari, *Journal of Micromechanics and Microengineering*, 30 (2020) 075001.
40. H. Savaloni, R. Savari and S. Abbasi, *Current Applied Physics*, 18 (2018) 869.
41. G. Gnana Kumar, S.-H. Chung, T. Raj Kumar and A. Manthiram, *ACS applied materials & interfaces*, 10 (2018) 20627.
42. J. Wang, Q. Zhao, H. Hou, Y. Wu, W. Yu, X. Ji and L. Shao, *RSC advances*, 7 (2017) 14152.
43. Y. Gao and I. Kyriatzi, *Bioconjugate Chemistry*, 19 (2008) 1945.
44. S. Smith, K. Goode, M. Delaney, A. Struzyk, N. Tansey and M. Frey, *Nanomaterials*, 10 (2020) 2142.

45. S. Bakshi, A. Zakharchenko, S. Minko, D.M. Kolpashchikov and E. Katz, *Magnetochemistry*, 5 (2019) 24.
46. C.E. Campiglio, N. Contessi Negrini, S. Farè and L. Draghi, *Materials*, 12 (2019) 2476.
47. A.H. Haghghi, M.T. Khorasani, Z. Faghih and F. Farjadian, *Heliyon*, 6 (2020) e03677.
48. M.D. Gholami, F. Theiss, P. Sonar, G.A. Ayoko and E.L. Izake, *Analyst*, 145 (2020) 5508.

© 2021 The Authors. Published by ESG (www.electrochemsci.org). This article is an open access article distributed under the terms and conditions of the Creative Commons Attribution license (<http://creativecommons.org/licenses/by/4.0/>).